ACS APPLIED MATERIALS & INTERFACES

Research Article

www.acsami.org

Metal-Enhanced Fluorescence-Based Core–Shell Ag@SiO_2 Nanoflares for Affinity Biosensing via Target-Induced Structure Switching of Aptamer

Lu Lu,[†,‡] Yunxia Qian,[†,‡] Lihui Wang,[†,‡] Keke Ma,[†,‡] and Yaodong Zhang*[,†,‡]

[†]Key Laboratory of Applied Surface and Colloid Chemistry of Ministry of Education and [‡]Key Laboratory of Analytical Chemistry for Life Science of Shaanxi Province, School of Chemistry and Chemical Engineering, Shaanxi Normal University, Xi'an 710062, China

Supporting Information

ABSTRACT: One of the great challenges in metal-enhanced fluorescence (MEF) technology is the achievement of distance modulation with nanometer accuracy between the fluorophore and metal surface to obtain maximum enhancement. We propose an MEF-based core–shell Ag@SiO_2 nanoflare for distance control via the thickness of silica shell with cooperation of DNA hybridization. The nanoflare contains a 50 nm spherical silver nanoparticle (Ag NP) core, a 8 nm silica shell, and cyanine (Cy5)-labeled aptamer hybridized with a complementary DNA (cDNA) immobilized onto the shell surface. The formation of the Cy5-labeled aptamer/cDNA duplex on the Ag@SiO_2 NP surface results in the confinement of Cy5 to the shell surface and an increase in the fluorescence of Cy5 with a 32-fold enhancement factor in bulk solution (signal-on). In the presence of affinity-binding targets, the Cy5-labeled aptamers confined onto the Ag@SiO_2 NP surface dissociate from their cDNA into the solution because of structure switching. The target-induced release of aptamer leads to a reduction in the enhanced fluorescence signal of the labeled Cy5 moiety (signal-off). Thus, the nanoflare can be used as a sensor for target recognition. Using adenosine-5′-triphosphate (ATP) aptamer, detection of ATP has a linear response from 0 to 0.5 mM and a detection limit of 8 μM. With various types of DNA probes immobilized onto the core–shell Ag@SiO_2 NPs, the MEF-based nanoflare has provided an effective platform for the detection and quantification of a broad range of analytes, such as mRNA regulation and detection, cell sorting, and gene profiling.

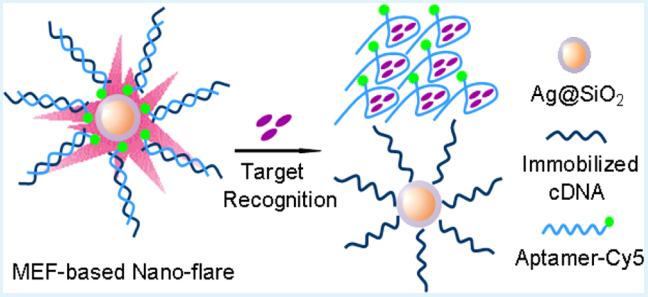

KEYWORDS: *metal-enhanced fluorescence, core–shell nanoparticle, silver nanoparticle, silica, aptamer, adenosine-5′-triphosphate*

1. INTRODUCTION

Metal-enhanced fluorescence (MEF) is an emerging technology that is expected to be extensively used in fluorescence-based applications in biomedicine and biotechnology.[1,2] MEF depends on the interactions of the excited-state fluorophores with the surface plasmon resonance of metal particles.[3] Aside from the reduced lifetime for the fluorophore on the metal nanoparticle (NP), the NP is capable of enhancing the local electromagnetic radiation field near the emitter, increasing the possibility of its excitation.[4−6] MEF is affected by numerous factors such as the type of metal NPs, size and morphology of the NPs, spatial distance between the fluorophore and NP surface,[7] and quantum yield of fluorophores.[8] Among these factors, the distance dependence is important in the fluorescence enhancement, in particular, the maximum enhancement at 7−10[9] and 5−11 nm.[10] Several techniques may be applied to adjust the distance between NPs and fluorophores. These techniques can be mainly classified into two categories based on the materials used for distance modulation. One method involves the use of protein (enzyme) or DNA molecules as the spacer layer. For instance, a complex was designed using human serum albumin as a spacer layer between the gold (Au) nanoshells and the fluorophore IR800.[10] Fluorescein-labeled DNA scaffolds of different lengths and covalently bound to silver (Ag) nanodeposits were used, and the distance dependence of the MEF effect has been experimentally measured.[11] We recently described a method for distance control between the Au NP and the fluorophore using acetylcholinesterase.[12] Although these spacer layers are convenient to create, they were not rigid enough to obtain accurate distance control. A SiO_2 matrix was used as a shell around the Ag core for distance control. This strategy provides three features:[13] (1) various available methods to conjugate the silica layer with biomolecules or fluorophores; (2) an adjustable thickness of the silica shell by simply controlling the amount of chemicals (e.g., tetraethylorthosilicate); (3) a protective layer of the Ag core from the distance between doped fluorophores and Ag NPs.[14] Core–shell structures effectively improve the stability of Ag nanostructures[15] and offer a rigid spacer to modulate the distance between the metal NPs and fluorophore

Received: November 7, 2013
Accepted: January 22, 2014
Published: January 30, 2014

   dx.doi.org/10.1021/am4049942 | ACS Appl. Mater. Interfaces 2014, 6, 1944−1950

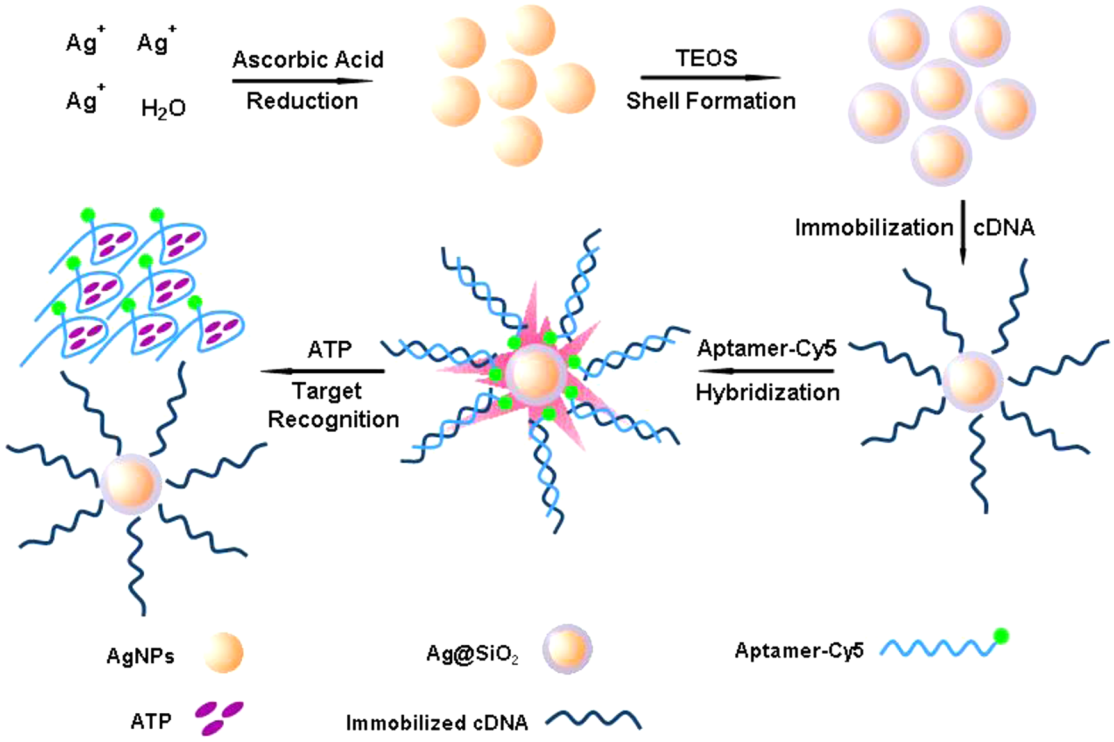

Figure 1. Schematic illustration of the preparation of MEF-based core−shell $Ag@SiO_2$ nanoflares and ATP detection.

to optimize the fluorescence efficiency.[16] In these methods, the fluorophores were usually doped into the silica shell to enhance fluorescence.[13,17] However, all doping methods can only obtain the average distance rather than the accurate distance. An interesting adsorption method for distance control has recently been developed and used for pH assay on the basis that the negatively charged fluorophores were absorbed onto the positively charged surface of a core−shell $Ag@SiO_2$ nanocomposite via electrostatic interactions. However, the assay has to be optimized because the desorption effects of the absorbed fluorophores resulted in a high background fluorescence signal.[18]

In this study, we designed and prepared an MEF-based core−shell $Ag@SiO_2$ nanoflare to develop a simple, efficient biosensing platform. As illustrated in Figure 1, a core−shell $Ag@SiO_2$ nanocomposite comprising an Ag NP core and a silica shell spacer with precise thickness was first synthesized. A complementary DNA (cDNA) probe modified with $-NH_2$ at the 5′ end was then immobilized onto the surface of the silica shell and hybridized with the target-binding aptamer labeled with Cy5 at the 3′ end. Thus, the fluorophore Cy5 was driven and confined to the silica surface via DNA hybridization, and the distance between the fluorophore and Ag NP was controlled by the thickness of the silica shell. The Cy5 was driven to close proximity with the shell surface, and its fluorescence was considerably increased because of the MEF (fluoresence turn-on). In the presence of analytes, the Cy5-labled aptamer bound with the affinity ligand and was released from the surface, resulting in a reduction of its fluorescence intensity (fluoresence turn-off).

Adenosine-5′-triphosphate (ATP), as the major source of chemical energy in living organisms, is involved with various kinds of vital movement.[19] Detection of the ATP levels can be extremely useful for metabolic studies in cell biology, as well as clinical diagnostics, and is thus highly important in detecting and monitoring the ATP concentration in aqueous media. Traditional methods, such as chromatographic,[20] electrochemical,[21] and bioluminometric approaches,[19] have been developed for accurate ATP detection. However, these methods are time-consuming or involved in complex chemical/enzymatic reactions.

Aptamers are a kind of nucleic acid and can bind with their respective ligands with high affinity and selectivity.[22−24] Because of the specific binding between the selected aptamer and ATP, the detection strategy of ATP based on aptamer has attracted much interest.[25,26] A series of fluorescent and electrochemical strategies have been established depending on aptamer-labeled fluorophores or electroactive tags to convert the specific binding reactions into detectable signals.[27,28] Some aptamer-based fluorescence methods for ATP detection include the molecular beacon approach and the structure switching/fluorescence−dequenching mechanism. The method based on a molecular beacon[29] commonly requires a dual-labeled aptamer that results in a distance change of the fluorophore and quenching induced by aptamer folding. The structure switching/fluorescence−dequenching[30] method markedly separates the quencher-labeled DNA from the labeled fluorophore, which results in increased fluorescence because the aptamer sequence switches to an aptamer/target complex. A Au NP was functionalized with a dense monolayer of ATP aptamers hybridized with cDNA labeled with fluorescent reporters. As the probes bind selectively to ATP, the fluorescent reporters are released and indicate the presence of target molecules.[31] As a proof of concept, the designed and prepared MEF-based core−shell $Ag@SiO_2$ nanoflare was used for a simple, efficient detection of ATP.

2. EXPERIMENTAL SECTION

2.1. Materials and General Methods. Silver nitrate ($AgNO_3$), tetraethylorthosilicate (TEOS), and 2,4,6-trichloro-1,3,5-triazine were

dx.doi.org/10.1021/am4049942 | ACS Appl. Mater. Interfaces 2014, 6, 1944−1950

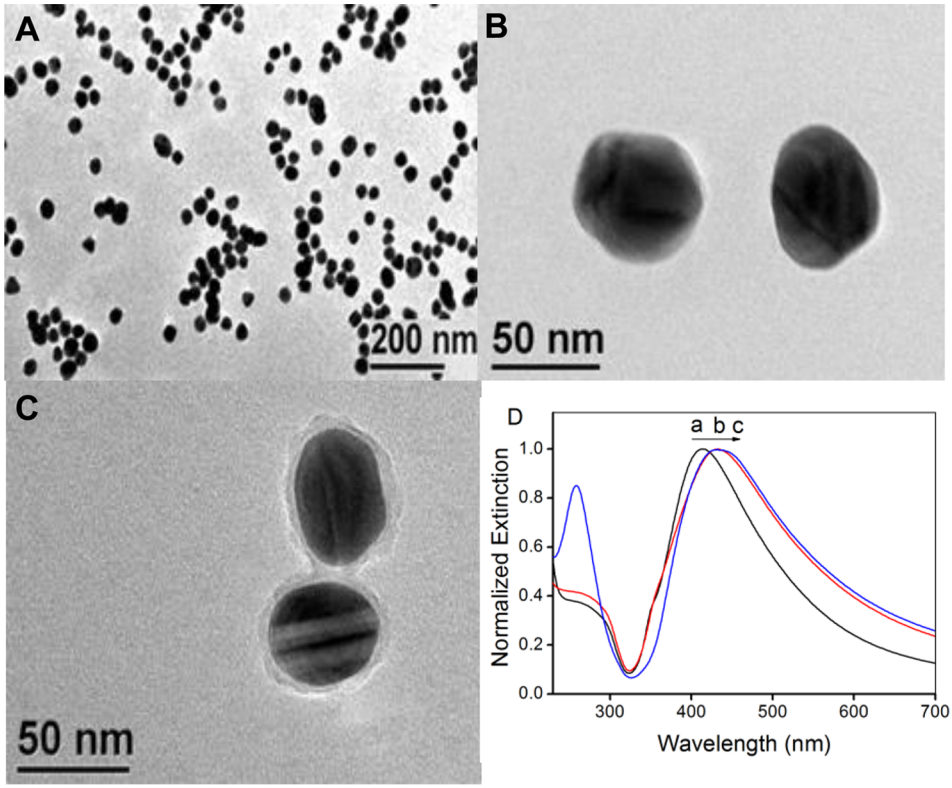

Figure 2. TEM images of the prepared Ag NPs with an average diameter of 50 nm (A and B) and core–shell Ag@SiO_2 NPs with 8 nm shell thickness (C). Normalized extinction spectra (D) of Ag NPs (curve a), Ag@SiO_2 (curve b), and Ag@SiO_2 immobilized with cDNA (curve c).

purchased from Sigma-Aldrich (Shanghai, China). (3-Aminopropyl)-triethoxysilane (3-APTS) was purchased from Alfa Aesar (Tianjing, China). 5′-$NH_2(CH_2)_6$-ACC TTC CTC CGC AAT ACT CCC CCA GGT-3′ (cDNA), 5′-ACC TGG GGG AGT ATT GCG GAG GAA GGT-Cy5-3′ (ATP-binding aptamer), adenosine-5′-triphosphate (ATP), guanosine 5′-triphosphate (GTP), cytosine 5′-triphosphate (CTP), and uridine 5′-triphosphate (UTP) were obtained from Shanghai Sangon Biotechnology Co. Ltd. (Shanghai, China). Other chemicals were purchased from Sinopharm Chemical Reagent Co., Ltd. (Shanghai, China).

Transmission electron microscopy (TEM) images of NP and nanocomposite specimens were recorded with a JEM-2100 transmission electron microscope (JEOL Co., Ltd., Japan) at an accelerating voltage of 100 kV. Absorption and emission spectra of all NP and nanocomposite samples were obtained with a PerkinElmer Lambda 35 UV–vis spectrometer and a PerkinElmer LS 55 fluorescence spectrometer (PerkinElmer, England), respectively. Circular dichroism (CD) spectra were obtained on a Chirascan CD spectrometer (Applied Photophysics, England).

2.2. Preparation of Core–Shell Ag@SiO_2 NPs. Ag NPs were first synthesized according to the literature.[32] Core–shell Ag@SiO_2 NPs were then obtained according to the literature[13] with slight modification. Briefly, 1 mL of a Ag colloid solution was mixed with 12.5 mL of isopropyl alcohol and 1.25 mL of deionized water under vigorous stirring. After the addition of 0.2 mL of 30% $NH_3 \cdot H_2O$, 5 μL of a TEOS solution with a concentration of 20% was immediately added into the mixed reactants. The reaction was carried out under agitation for 30 min at room temperature (RT), and then the products were aged without stirring at 4 °C overnight. The silica-coated Ag NP suspension was washed three times with a water and ethanol mixture (5:4) and centrifuged at 6000 rpm for 20 min. Finally, the core–shell Ag@SiO_2 NPs were resuspended in water, and the thickness of the silica shell was determined by TEM.

2.3. Immobilization of cDNA onto Ag@SiO_2 NPs. Immobilization of cDNA onto Ag@SiO_2 NPs was performed according to the literature[33] with slight modification (see the Supporting Information, Figure S1). The prepared Ag@SiO_2 NPs were mixed with 600 μL of absolute ethanol, and 400 μL of 3-APTS was then added after 5 min of stirring. The mixture was shaken for 2 h at RT and quickly heated at 50 °C for 1 h. The mixture was centrifuged and washed with ethanol and acetonitrile after the mixture was cooled to RT. Then, 1 mL of 0.2 M 2,4,6-trichloro-1,3,5-triazine (dissolved in acetonitrile) was mixed with the NPs and allowed to react for 2 h at RT. After the mixture was centrifuged, it was washed three times with acetonitrile and two times with ethanol, ultrapure water, and 0.05 M sodium borate buffer (pH 8.4) successively and then dispersed in the borate buffer (a mixture of 90 μL of 2 M NaCl and 90 μL of 0.05 M sodium tetraborate decahydrate, pH 8.4). Finally, the cDNA probes (500 μL, 1 μM) were added and incubated for 14 h at RT for immobilization of cDNA onto Ag@SiO_2 NPs.

2.4. Preparation of Core–Shell Ag@SiO_2 Nanoflares. To prepare the core–shell Ag@SiO_2 nanoflares, the Cy5-labeled aptamer hybridized with cDNA was immobilized onto Ag@SiO_2 NPs. Hybridization was performed in solution as previously described with slight modification.[34] The Ag@SiO_2 NPs immobilized with cDNA were suspended in 500 μL of a hybridization buffer (50 mM Tris-HCl, 0.1% Tween-20, 1 M NaCl, pH 8.4), followed by the addition of 50 μL of 10 μM Cy5-labeled aptamer (in 0.05 M borate buffer, pH 8.4). The mixture was shaken and incubated at RT for 2 h. Then, the NPs were washed with the hybridization buffer by three rounds of centrifugation to remove the free aptamers. The supernatant was collected after centrifugation for measurement of the absorbance at 260 nm and calculation of the hybridization ratio. The prepared nanoflares were collected and redispersed in 1 mL of the hybridization buffer for further use and measurement.

2.5. ATP Detection Using MEF-Based Core–Shell Ag@SiO_2 Nanoflare. Various concentrations of ATP (0 to 2.0 mM) were added to the prepared core–shell Ag@SiO_2 nanoflare solution (20 mM Tris, 5 mM $MgCl_2$, 300 mM NaC1, pH 7.6). The mixture was incubated at 45 °C for 30 min. Then, the fluorescence spectra were recorded, and the fluorescence intensities at 670 nm were determined. The experiments for the selectivity test were performed with the ATP

analogues GTP, CTP, and UTP with concentrations of 0.5 mM under identical conditions.

2.6. Sensing ATP in Human Blood. Samples of fresh blood were obtained from the antecubital vein of three healthy volunteers at a local hospital and collected using ethylenediaminetetraacetic acid for anticoagulation. Samples were subjected to alkaline extraction of nucleotides according to the method described by Stocchi with slight modification.[35] A total of 1.0 mL of blood was added to 1.0 mL of ice cold 0.5 M KOH, incubated for 10 min at 4 °C, and then filtered with a size-exclusion spin column (10 kDa cutoff, Amicon) by centrifugation (2500*g*, 20 min, and 4 °C). The clear ultrafiltered solution was collected and adjusted to pH 7.6 with 1 M HCl, then diluted to 5.0 mL with a detection buffer (20 mM Tris, 5 mM $MgCl_2$, 300 mM NaC1, pH 7.6), and used for ATP analysis using a core−shell Ag@SiO_2 nanoflare. For the recovery test, known quantities of ATP (400 μM) were added to the blood samples and alkaline extraction was immediately performed.

3. RESULTS AND DISCUSSION

3.1. Preparation of a Core−Shell Ag@SiO_2 NP as the Matrix for MEF. Ag was selected to build the NP core because it has been considered to be a preferred fluorescence enhancer among the noble metals because of its high scattering efficiency and narrow plasmon resonance band. The quenching and enhancement of metal NPs were empirically described[8] using the radiating plasmon model in which quenching results from the absorption component in the extinction spectrum, whereas enhancement reflects the scattering contribution, with relative proportions depending on the size, shape, and composition of the NPs.[36] Lakowicz et al. proved that the diameter of Ag NPs is optimal from 50 to 70 nm to provide the strength distribution of the enhanced electromagnetic field of localized surface plasmon resonance (LSPR) and the depression of competitive quenching.[37] The diameter of the Ag core was 50 nm for all of the preparations in this work, a size that has been shown to be suitable for MEF and the radiating plasmon model.[37−39] The preparation of core−shell Ag@SiO_2 nanocomposites was undertaken in two steps: (1) spherical 50 nm Ag NPs were prepared by a reduction of $AgNO_3$ by ascorbic acid; (2) the prepared Ag NPs were homogeneously coated with an 8 nm silica shell.

Several reductants, such as sodium borohydride,[40] sodium citrate,[41] or ascorbic acid,[42] can be used in a reduction of $AgNO_3$ to obtain the Ag NPs in an aqueous solution. Given the high reactivity of sodium borohydride, which can induce an explosive nucleation process, the products were usually small spherical Ag NPs (<10 nm). When sodium citrate was used as the reductant, there were some unexpected rodlike Ag NPs that mixed with the spherical particles because of the poor balance of nucleation and growth processes.[43] Thus, we selected ascorbic acid as the reductant with suitable reactivity to regulate the nucleation and growth processes of the Ag NPs.

The morphology of final prepared Ag NPs was determined by TEM. Parts A−C of Figure 2 display TEM images showing generally spherical and proportioned Ag NPs with a diameter at 50 ± 3 nm. Thus, the resulting Ag NPs are expected to indicate highly enhanced fluorescence. The prepared Ag NPs can be homogeneously coated with a silica shell by carefully adjusting the amount of TEOS and $NH_3{\cdot}H_2O$ in the diluted isopropyl alcohol solution. Figure 2C shows as-fabricated Ag@SiO_2 with a silica shell thickness of 8 ± 1 nm. Given the increase in the local refractive index of the silica shell and the decreased plasmon oscillation energy,[44] a red shift of 14 nm (from 419 to 433 nm) in the plasmon resonance band was evident compared with that of uncoated Ag NPs, which was shown in the UV−vis spectra (Figure 2D). This result is in good agreement with a previous report.[45] Thus, appropriate Ag@SiO_2 NPs were successfully synthesized, and the distance between the resulting Ag NPs and fluorophore was well controlled with relatively high uniformity.

3.2. Fabrication of MEF-Based Core−Shell Ag@SiO_2 Nanoflares. The detection strategy started with the immobilization of cDNA on the core−shell Ag@SiO_2 surface, followed by hybridization of the Cy5-labeled aptamer with cDNA-immobilized NPs (Figure 1). We selected 2,4,6-trichloro-1,3,5-triazine, which has better surface chemistry in covalent attachment of oligonucleotides to silica NPs, to functionalize Ag@SiO_2 NPs.[33] A triazine-functionalized core−shell Ag@SiO_2 surface was accomplished via a two-step process. First, 3-APTS was added to the ethanol solution of Ag@SiO_2 NPs to generate an amine-modified surface. Second, 2,4,6-trichloro-1,3,5-triazine was used to generate a triazine-functionalized surface for further modification with amino-terminated cDNA. The successful immobilization of cDNA on the NP surface was observed by the absorbance at 260 nm of Ag@SiO_2 NPs after cDNA immobilization (Figure 2D, curve c). The coverage density was calculated to be 420 ± 38 cDNA per Ag@SiO_2 (see the Supporting Information, section S2). Only a slight red shift in the plasmon resonance band was determined compared with that of Ag@SiO_2 NPs without cDNA immobilization (Figure 2D).

After successful surface modification, incubation of immobilized cDNA with the Cy5-labeled aptamer in the hybridization buffer resulted in the formation of DNA duplexes on the NP surface and approach of Cy5 to the shell surface of Ag@SiO_2 NPs. Cy5 is a common fluorescent dye molecule that strongly absorbs at 640 nm and emits at 670 nm. This molecule was chosen as the fluorophore not only because Cy5 is one of the common fluorescent labeling reagents but also because the brightest fluorescence was observed from dyes attached to metal NPs that have LSPR scattering peaks 40−120 meV higher in energy than the emission peak of the fluorophore.[46,47] According to the amount of cDNA immobilized onto Ag@SiO_2 NPs, the Cy5-labeled aptamer was added into the hybridization buffer. The hybridization efficiency can be calculated by means of measuring the absorbance of the aptamer solution before hybridization and that of the collected supernatant after hybridization. When the added number of Cy5-labeled aptamers was 3.0×10^{14} in the hybridization solution, the hybridized aptamer number on Ag@SiO_2 NPs immobilized with cDNA was calculated to be 1.2×10^{13}, which corresponded to (93 ± 8)% of the immobilized cDNA that participated in the hybridization (see the Supporting Information, section S3).

To estimate the MEF abilities of as-prepared core−shell Ag@SiO_2 NP nanoflares, the fluorescence enhancement was investigated and characterized using fluorescence enhancement factor F ($F = I_{nanoflares}/I_{control}$, where $I_{nanoflares}$ denotes the fluorescence intensity of the peak at 670 nm of the as-prepared MEF-based Ag@SiO_2 NP nanoflares and $I_{control}$ denotes the fluorescence intensity of the peak at 670 nm of the control sample, which consisted of core−shell Ag@SiO_2, cDNA, and the Cy5-labeled aptamer, all with similar amounts compared with the prepared nanoflare. The fluorescence intensity increased by 32 times (n = 3) when the concentrations of Ag@SiO_2, cDNA, and the Cy5-labeled aptamer in the control sample were 0.51×10^{-10}, 2.1×10^{-8}, and 1.9×10^{-8} M,

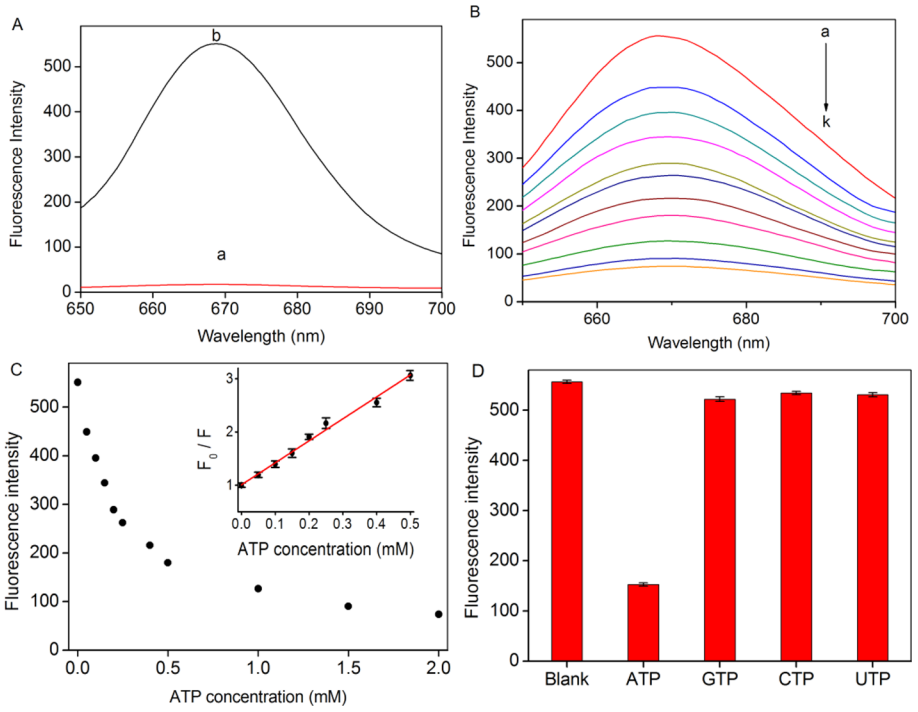

Figure 3. (A) Fluorescence spectra of the nanoflare (curve a) and the control sample (curve b). (B) Emission spectra of the nanoflare in the presence of various concentrations of ATP. λ_{ex} = 640 nm, λ_{em} = 670 nm, and Ca-k (ATP) = 0.0, 0.05, 0.1, 0.15, 0.2, 0.25, 0.4, 0.5, 1.0, 1.5, and 2.0 mM. (C) Plot of the fluorescence intensity at 670 nm of the nanoflare versus the various ATP concentrations. The inset shows F_0/F versus the ATP concentration from 0.0 to 0.5 mM. F_0 and F are the fluorescence intensities in the absence and presence of ATP, respectively. (D) Selectivity test for ATP. The ATP concentration is 0.5 mM. Each data point represents the average value of three independent experiments with error bars indicated.

respectively (Figure 3A), which were obtained from calculations of the number of immobilized cDNA and the hybridization ratio. Notably, using highly toxic KCN to etch the Ag core for preparation of the control sample in this homogeneous assay format is not necessary like in other methods.[13,48] The largest enhanced factor was obtained in bulk solution by far and can be further increased by adjusting the amount of dye-labeled aptamer in the solution to reduce the background signal, by optimizing the topology, dimensions, and composition of NPs or by selecting more appropriate fluorescent molecules.

The stability of the prepared MEF-based core−shell Ag@SiO_2 nanoflares was further investigated. To remove the free aptamer in solution, the nanoflares were further washed three times with the hybridization buffer and hardly any fluorescence was measured in the supernatant. Therefore, the hybridized Cy5-labled aptamers were not released into the solution. In addition, upon incubation of the nanoflares at different temperatures, the fluorescence of the NP probe solution remained constant when the temperature was changed from 25 to 50 °C, indicating that no aptamer was released into the solution. This phenomenon is due to the high melting temperature of the aptamer/DNA duplex (T_m = 66.4 °C, calculated with IDT *OligoAnalyzer 3.1*, http://www.idtdna.com/). The results confirm that cDNA-immobilized Ag@SiO_2 NPs can function as an ideal tool for the capture of aptamer and lower the background signal.

3.3. Assay Performance on ATP. A DNA aptamer that binds adenosine and ATP selected by Huizenga and Szostak[49] was used in this work. To test the affinity biosensing of target molecules, MEF-based Ag@SiO_2 NP nanoflares (0.51×10^{-10} M) in the hybridization buffer were titrated with different concentrations of ATP (Figure 3B). As shown in Figure 3C, the plot of the fluorescence intensity of the nanoflares versus the ATP concentrations showed a dynamic range from 0 to 0.5 mM with a detection limit as low as 8 μM (signal/noise ratio = 3). Therefore, the assay method is sensitive to ATP concentrations that are commonly found in cells (0.1−3.0 mM).[50,51] The sensor could be reused after washing with the hybridization buffer by centrifugation and hybridizing with the Cy5-labeled aptamer. Although the "on-off" format was applied for biosensing, the final "signal-off" detecting platform was used to measure the target. Thus, other quenchers or environmental stimuli can also lead to fluorescence turn-off and cause false-positive signals.

To evaluate the specificity of the nanoflare sensor, control experiments were conducted by incubating the nanoflares in the hybridization buffer containing various concentrations of ATP analogues, including CTP, GTP, and UTP (Figure 3D). Exposure to these ATP analogues induced a negligible response of the nanoflare sensor, strongly demonstrating that the nanoflares can discriminate between ATP and these analogues. These results are consistent with a selective target binding ability.

Three fresh blood samples from healthy individuals were provided by a local hospital, ruled by the ethical committee. After alkaline extraction, the concentrations of ATP were determined to be 467, 481, and 512 μM, respectively (Table 1). The values are slightly higher than those reported in previous works.[50,52] The possible reason is that adenosine, adenosine-5′-diphosphate, and adenosine-5′-monophosphate can also bind with the aptamer, even those compounds with lower amounts compared to ATP in human blood. For further evaluation of the validity of the proposed method, known quantities (400

Table 1. Analytical Results of ATP Determination in Human Blood[a]

sample no.	measured (μM)	added (μM)	recovered (μM)	recovery (%)	RSD (%)
1 (woman)	467	400	843	94	6.5
2 (woman)	481	400	837	89	8.4
3 (man)	512	400	880	92	6.9

[a]The human blood samples were treated with alkaline extraction. n = 3.

μM) of ATP were added to the blood samples, and the recoveries were determined to be 89–94% (Table 1). These results clearly suggest that the assay could be applied to detection of ATP in a real sample.

The ATP binding switches the Cy5-labeled aptamer/cDNA duplex to an aptamer/ATP complex, which forces dissociation of the Cy5-labeled aptamers from their respective cDNA into the solution, resulting in a decrease in MEF and a reduction in the fluorescence signal. This viewpoint was shown by CD measurements. Figure 4 shows that, in the absence of ATP, a

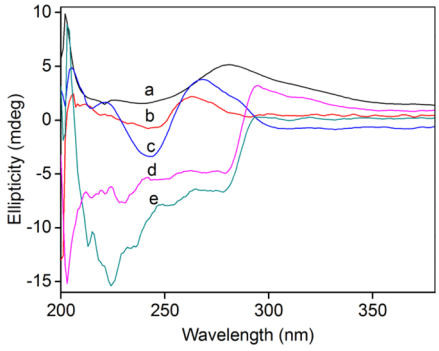

Figure 4. CD spectra of solutions of (a) cDNA, (b) ATP aptamer, (c) cDNA + ATP aptamer, (d) cDNA + ATP aptamer + ATP, and (e) ATP aptamer + ATP. The concentrations of cDNA, ATP aptamer, and ATP are 5, 5, and 50 μM, respectively.

weak positive band near 270 nm and a weak negative band at 245 nm are found in the CD spectrum of the solution of the Cy5-labeled aptamer and cDNA (curve c), which is a main characteristic of a B-type duplex conformation.[53] A significant change in the ellipticity (millidegrees) was observed in the presence of ATP; especially, a positive band near 285 nm was determined in its CD spectrum, implying that the antiparallel quadruplex structures (curve d) are formed by ATP induction.[54] The structure switching is also confirmed by the control experiments of CD spectra (curves a, b, and e).

4. CONCLUSIONS

We have demonstrated the design of plasmonic core–shell Ag@SiO_2 nanoflares. We precisely controlled the distance between the fluorophore and Ag NPs by modulating the thickness of the silica shell and confining the fluorophore to the shell surface through DNA hybridization. Thus, distance control with nanometer accuracy between the fluorophore and metal surface has been realized. The highly efficient fluorescence enhancement properties of Ag, high signaling of the "on-off" format, and low background fluorescence were beneficial in overcoming many of the challenges in creating sensitive and effective fluorescent probes. The 32-fold fluorescence enhancement factor in a bulk solution was obtained under homogeneous assay conditions. Using an ATP-binding aptamer, the rational design of plasmonic core–shell Ag@SiO_2 nanoflares can be used for rapid detection and quantification of ATP with high sensitivity and selectivity. The proposed platform is generally applicable to any aptamer and corresponding biomolecules. Future work will include the application of various types of immobilized DNA probes for mRNA regulation and detection, quantitation of biomolecules in living cells, cell sorting, and gene profiling.[55,56]

■ ASSOCIATED CONTENT

Supporting Information

Calculation of the number of cDNAs immobilized onto the Ag@SiO_2 NP, calculation of the hybridization ratio of surface-immobilized cDNA, and Figure S1. This material is available free of charge via the Internet at http://pubs.acs.org.

■ AUTHOR INFORMATION

Corresponding Author

*Tel.: +86-29-81530726. Fax: +86-29-81530727. E-mail: ydzhang@snnu.edu.cn.

Notes

The authors declare no competing financial interest.

■ ACKNOWLEDGMENTS

We express our gratitude to Prof. Dr. C. Zhang for his kind help. This work was supported by the National Natural Science Foundation of China (Grant 21275097), the Fundamental Research Fund for the Central Universities (Grant GK201303001), and the Program for Changjiang Scholars and Innovative Research Team in University (IRT 1070).

■ REFERENCES

(1) Aslan, K.; Gryczynski, I.; Malicka, J.; Matveeva, E.; Lakowicz, J. R.; Geddes, C. D. *Curr. Opin. Biotechnol.* **2005**, *16*, 55–62.
(2) Li, H.; Chen, C. Y.; Wei, X.; Qiang, W.; Li, Z.; Cheng, Q.; Xu, D. *Anal. Chem.* **2012**, *84*, 8656–8662.
(3) Bharill, S.; Chen, C.; Stevens, B.; Kaur, J.; Smilansky, Z.; Mandecki, W.; Gryczynski, I.; Gryczynski, Z.; Cooperman, B. S.; Goldman, Y. E. *ACS Nano* **2011**, *5*, 399–407.
(4) Kühn, S.; Håkanson, U.; Rogobete, L.; Sandoghdar, V. *Phys. Rev. Lett.* **2006**, *97*, 017402.
(5) Karolin, J. O.; Geddes, C. D. *J. Fluoresc.* **2012**, *22*, 1659–1662.
(6) Ray, K.; Lakowicz, J. R. *J. Phys. Chem. C* **2013**, *117*, 15790–15797.
(7) Saboktakin, M.; Ye, X.; Oh, S. J.; Hong, S. H.; Fafarman, A. T.; Chettiar, U. K.; Engheta, N.; Murray, C. B.; Kagan, C. R. *ACS Nano* **2012**, *6*, 8758–8766.
(8) Lakowicz, J. R. *Anal. Biochem.* **2005**, *337*, 171–194.
(9) Lakowicz, J. R.; Geddes, C. D.; Gryczynski, I.; Malicka, J.; Gryczynski, Z.; Aslan, K.; Lukomska, J.; Matveeva, E.; Zhang, J.; Badugu, R.; Huang, J. *J. Fluoresc.* **2004**, *14*, 425–441.
(10) Bardhan, R.; Grady, N. K.; Cole, J. R.; Joshi, A.; Halas, N. J. *ACS Nano* **2009**, *3*, 744–752.
(11) Dragan, A. I.; Bishop, E. S.; Casas-Finet, J. R.; Strouse, R. J.; McGivney, J.; Schenerman, M. A.; Geddes, C. D. *Plasmonics* **2012**, *7*, 739–744.
(12) Zhang, Y.; Hei, T.; Cai, Y.; Gao, Q.; Zhang, Q. *Anal. Chem.* **2012**, *84*, 2830–2836.
(13) Aslan, K.; Wu, M.; Lakowicz, J. R.; Geddes, C. D. *J. Am. Chem. Soc.* **2007**, *129*, 1524–1525.
(14) Asian, K.; Lakowicz, J. R.; Szmacinski, H.; Geddes, C. D. *J. Fluoresc.* **2004**, *14*, 677–679.
(15) Mahmoudi, M.; Shokrgozar, M. A. *Chem. Commun.* **2012**, *48*, 3957–3959.

(16) Zhang, F.; Braun, G. B.; Shi, Y.; Zhang, Y.; Sun, X.; Reich, N. O.; Zhao, D.; Stucky, G. *J. Am. Chem. Soc.* **2010**, *132*, 2850−2851.
(17) Arifin, E.; Lee, J. K. *Bull. Korean Chem. Soc.* **2013**, *34*, 539−544.
(18) Bai, Z.; Chen, R.; Si, P.; Huang, Y.; Sun, H.; Kim, D.-H. *ACS Appl. Mater. Interfaces* **2013**, *5*, 5856−5860.
(19) Perez-Ruiz, T.; Martinez-Lozano, C.; Tomas, V.; Martin, J. *Anal. Bioanal. Chem.* **2003**, *377*, 189−194.
(20) Stratford, M. R.; Dennis, M. F. *J. Chromatogr. B* **1994**, *662*, 15−20.
(21) Compagnone, D.; Guilbault, G. G. *Anal. Chim. Acta.* **1997**, *340*, 109−113.
(22) Tuerk, C.; Gold, L. *Science* **1990**, *249*, 505−510.
(23) Ellington, A. D.; Szostak, J. W. *Nature* **1990**, *346*, 818−822.
(24) Cho, E. J.; Lee, J. W.; Ellington, A. D. *Annu. Rev. Anal. Chem.* **2009**, *2*, 241−264.
(25) Cong, X.; Nilsen-Hamilton, M. *Biochemistry* **2005**, *44*, 7945−7954.
(26) Lu, C. H.; Li, J.; Lin, M. H.; Wang, Y. W.; Yang, H. H.; Chen, X.; Chen, G. N. *Angew. Chem., Int. Ed.* **2010**, *49*, 8454−8457.
(27) Li, Y.; Qi, H.; Peng, Y.; Zhang, C. *Electrochem. Commun.* **2007**, *9*, 2571−2575.
(28) Radi, A. E.; Acero Sanchez, J. L.; Baldrich, E.; O'Sullivan, C. K. *J. Am. Chem. Soc.* **2006**, *128*, 117−124.
(29) Tang, Z.; Mallikaratchy, P.; Yang, R.; Kim, Y.; Zhu, Z.; Wang, H.; Tan, W. *J. Am. Chem. Soc.* **2008**, *130*, 11268−11269.
(30) Nutiu, R.; Li, Y. *J. Am. Chem. Soc.* **2003**, *125*, 4771−4778.
(31) Zheng, D.; Seferos, D. S.; Giljohann, D. A.; Patel, P. C.; Mirkin, C. A. *Nano Lett.* **2009**, *9*, 3258−3261.
(32) Qin, Y.; Ji, X.; Jing, J.; Liu, H.; Wu, H.; Yang, W. *Colloids Surf., A* **2010**, *372*, 172−176.
(33) Steinberg, G.; Stromsborg, K.; Thomas, L.; Barker, D.; Zhao, C. *Biopolymers* **2004**, *73*, 597−605.
(34) Wang, Y.; Wang, Y.; Liu, B. *Nanotechnology* **2008**, *19*, 415605.
(35) Stocchi, V.; Cucchiarini, L.; Magnani, M.; Chiarantini, L.; Palma, P.; Crescentini, G. *Anal. Biochem.* **1985**, *146*, 118−124.
(36) Jain, P. K.; Lee, K. S.; El-Sayed, I. H.; El-Sayed, M. A. *J. Phys. Chem. B* **2006**, *110*, 7238−7248.
(37) Lakowicz, J. R.; Ray, K.; Chowdhury, M.; Szmacinski, H.; Fu, Y.; Zhang, J.; Nowaczyk, K. *Analyst* **2008**, *133*, 1308−1346.
(38) Aslan, K.; Leonenko, Z.; Lakowicz, J. R.; Geddes, C. D. *J. Fluoresc.* **2005**, *15*, 643−654.
(39) Naiki, H.; Masuhara, A.; Masuo, S.; Onodera, T.; Kasai, H.; Oikawa, H. *J. Phys. Chem. C* **2013**, *117*, 2455−2459.
(40) Ahmadi, T. S.; Wang, Z. L.; Green, T. C.; Henglein, A.; El-Sayed, M. A. *Science* **1996**, *272*, 1924−1926.
(41) Pillai, Z. S.; Kamat, P. V. *J. Phys. Chem. B* **2004**, *108*, 945−951.
(42) Sondi, I.; Goia, D. V.; Matijevic, E. *J. Colloid Interface Sci.* **2003**, *260*, 75−81.
(43) Dong, X.; Ji, X.; Wu, H.; Zhao, L.; Li, J.; Yang, W. *J. Phys. Chem. C* **2009**, *113*, 6573−6576.
(44) Bardhan, R.; Grady, N. K.; Halas, N. J. *Small* **2008**, *4*, 1716−1722.
(45) Evanoff, D. D.; White, R. L.; Chumanov, G. *J. Phys. Chem. B* **2004**, *108*, 1522−1524.
(46) Chen, Y.; Munechika, K.; Ginger, D. S. *Nano Lett.* **2007**, *7*, 690−696.
(47) Fu, Y.; Zhang, J.; Lakowicz, J. R. *J. Am. Chem. Soc.* **2010**, *132*, 5540−5541.
(48) Guo, L.; Guan, A.; Lin, X.; Zhang, C.; Chen, G. *Talanta* **2010**, *82*, 1696−1700.
(49) Huizenga, D. E.; Szostak, J. W. *Biochemistry* **1995**, *34*, 656−665.
(50) Traut, T. W. *Mol. Cell. Biochem.* **1994**, *140*, 1−22.
(51) Gorman, M. W.; Feigl, E. O.; Buffington, C. W. *Clin. Chem.* **2007**, *53*, 318−325.
(52) Bishop, C.; Rankine, D. M.; Talbott, J. H. *J. Biol. Chem.* **1959**, *234*, 1233−1237.
(53) Gratzer, W. B.; Hill, L. R.; Owen, R. J. *Eur. J. Biochem.* **1970**, *15*, 209−214.
(54) Ambrus, A.; Chen, D.; Dai, J.; Bialis, T.; Jones, R. A.; Yang, D. *Nucleic Acids Res.* **2006**, *34*, 2723−2735.
(55) Prigodich, A. E.; Seferos, D. S.; Massich, M. D.; Giljohann, D. A.; Lane, B. C.; Mirkin, C. A. *ACS Nano* **2009**, *3*, 2147−2152.
(56) Wu, C.; Chen, T.; Han, D.; You, M.; Peng, L.; Cansiz, S.; Zhu, G.; Li, C.; Xiong, X.; Jimenez, E.; Yang, C. J.; Tan, W. *ACS Nano* **2013**, *7*, 5724−5731.